LIMNOLOGY AND OCEANOGRAPHY
Letters

ASLO
Open Access

Limnology and Oceanography Letters 8, 2023, 867–875

doi: 10.1002/lol2.10345

LETTER

Coastal marine megaripple fields are metabolic hotspots with highly dynamic oxygen exchange

Peter Berg [1]*, *Markus Huettel* [2]

[1]Department of Environmental Sciences, University of Virginia, Charlottesville, Virginia, USA; [2]Department of Earth, Ocean and Atmospheric Science, Florida State University, Tallahassee, USA

Scientific Significance Statement

Permeable sand megaripples are found in many coastal and shelf environments with strong currents, but little is known about their biochemical functioning, including their carbon cycling. This knowledge gap is largely rooted in the previous lack of methods for measuring undisturbed fluxes across the seafloor in high-energy settings. Over a shallow-water megaripple field, we used the aquatic eddy covariance technique to measure benthic oxygen fluxes under naturally varying environmental conditions (e.g., current, waves, and light). Our results show that the carbon cycling rates in the megaripple field are substantial, exceeding those reported for many shallow-water sediments.

Abstract

Megaripples are current-generated seafloor bedforms of well-sorted sand or gravel and wavelengths over 1 m. In this aquatic eddy covariance study, we measured large rates of benthic primary production and respiration for a shallow-water sandy megaripple field exposed to strong tidally driven currents and intense sunlight. Current and light were the main short-term drivers of a highly dynamic oxygen exchange. Daytime oxygen release as high as 300 mmol m^{-2} d^{-1} and nighttime oxygen uptake up to −100 mmol m^{-2} d^{-1} were likely sustained by current-driven transport of oxygen, nutrients, and organic matter (fuel) into and out of the sand and superimposed by rapid internal cycling. Seasonal differences in temperature (45%) and light (69%) between April and September were the main long-term drivers of substantially greater rates of gross primary production and respiration in September. The megaripples functioned as an intense metabolic hotspot with carbon cycling rates larger than those of most near-shore sediments.

Megaripples of highly permeable sand and gravel are common topographical features found globally on the seafloor from near-shore to deep-sea settings (Cacchione et al. 1987; Carling 1999; Gallagher 2003; Cuevas et al. 2013; Cheng et al. 2020). They are formed by strong bottom currents in high-energy environments, and are usually defined

*Correspondence: pb8n@virginia.edu

Associate editor: Daniel J. Conley

Author Contribution Statement: PB and MH designed and executed the field work together. PB extracted aquatic eddy covariance fluxes. PB and MH discussed and synthesized all results jointly. PB wrote the manuscript with input and comments from MH.

Data Availability Statement: Published data and metadata are available in the Environmental Data Initiative repository: https://doi.org/10.6073/pasta/d6e88492c91dcc16370ab55f34613686.

Additional Supporting Information may be found in the online version of this article.

as bedforms with wavelengths > 1 m (Ashley 1990) and crests oriented perpendicular to the regional peak flow direction (Bellec et al. 2019). In the coastal zone and inner shelf, megaripples are mainly found in areas with a large tidal range and areas where currents are amplified by land mass obstructions or underwater sills (Engelund and Fredsoe 1982; Carling 1999). In such dynamic environments, megaripple migration rates of 6.5–20 m yr^{-1} have been observed (van Dijk and Kleinhans 2005). In less dynamic environments, megaripples are produced during major storms and can then persist for years without significant change (Iacono and Guillén 2008).

The geology, including the formation and migration of megaripples and other larger topographic features like sandwaves and sandbanks have been studied extensively, partly because they represent a hazard to ship navigation (Collins et al. 1995; Poppe et al. 2008; Bellec et al. 2010). By using state-of-the-art high-resolution multibeam echosounder technology that resolves bedforms as small as 4-cm high, and advanced gridding and visualization software, illustrative color images of these seafloor features have been produced (Bellec et al. 2019). In contrast, virtually nothing is known about the biochemical functioning of megaripple fields. A major reason for this is that it is challenging to obtain realistic in situ benthic flux numbers using traditional methods in highly permeable sediment exposed to strong currents (Berg et al. 2013).

Our understanding of biochemical processes in smaller sand ripples (wavelength < 1 m) is well-established thanks to pioneering work initiated in the 1990s that visualized and documented how bottom currents drive both solutes and particles into the permeable sediment and create an environment favorable for intense microbial activity (Huettel and Gust 1992; Huettel et al. 1996; Ziebis et al. 1996). Decay products of this activity, including nutrients and dissolved inorganic carbon, are in turn flushed out of the sand, resulting in tight biogeochemical couplings between sand and the water above. Prior to this line of work, sandy sediments were viewed as sites of low metabolic activity due to their typically low organic matter content (Boudreau et al. 2001). In reality, they function as highly effective biocatalytical filters that rapidly transform the carbon they capture at rates on par with or exceeding those of typical muddy cohesive sediments (Huettel et al. 2014).

Similarities in topography, between megaripples and smaller sand ripples and the flow and its diversion over them that can drive solute and particle exchange with the water column, suggest that megaripples may be sites with high carbon transformation rates as their smaller counterpart. If so, and given how widespread megaripples are (Ashley 1990), they may have the potential to impact the carbon cycling and oxygen (O_2) dynamics in the environments where they are found. This knowledge gap motivated this study in which we present, as far as we know, the first metabolic measurements in a shallow-water sandy megaripple field. We used in situ benthic O_2 fluxes as a proxy for carbon transformation and relate the fluxes to environmental drivers such as light, current, and temperature. In addition, we used transect-measurements of ripple topography and O_2 concentration in the top sediment layer to argue that our benthic fluxes represent the O_2 exchange across the whole megaripple field.

All benthic O_2 fluxes were measured by aquatic eddy covariance (AEC), a technique that over the last 20 yrs has become a widely accepted and used approach for measuring underwater O_2 fluxes (Berg et al. 2003). The technique has several unique advantages over other flux methods, including its noninvasive nature (Lorrai et al. 2010), high temporal resolution (Rheuban and Berg 2013), and its ability to integrate over a large benthic surface (Berg et al. 2007). As it relies on direct measurements of the turbulent transport up from or down toward a benthic surface without "touching" it or disturbing the flow over it, the approach is well-suited for measuring fluxes where local environmental conditions (e.g., current, waves, and light) are major drivers of the benthic exchange (Attard et al. 2019; Long 2021; Berg et al. 2022).

Methods

Site description and visits

Our study site is a ~ 1 km long shallow-water megaripple field at the outlet of Choctawhatchee Bay in the northeastern Gulf of Mexico, Florida, USA (Fig. 1a). The average water depth along the center line of the megaripple field is ~ 3.6 m with a diurnal tidal variation of ~ 0.5 m. The megaripples have an average wavelength of ~ 18 m, an average height of ~ 0.45 m, and consist of well-sorted quartz sand with a median grain size of 145 μm and an average permeability of 5×10^{-11} m^2. The latter is about 50 times higher than the threshold of ~ 10^{-12} m^2 where flow-driven advective sediment–water exchange is considered to exceed that of molecular diffusion (Huettel et al. 2014).

Choctawhatchee Bay has several freshwater input sources with Choctawhatchee River being the largest. The megaripples in the bay outlet are periodically migrating toward the ocean during episodic extreme freshwater runoff associated with heavy rainstorms and outgoing tides when peak current velocities arise. This geomorphological pattern is evident from the typical asymmetric shape of the ripples visible in Google Earth (Fig. 1a; *see* also topography profile in Results). The megaripple field, particularly near the crests, is superimposed by smaller sand ripples and other rugosities (Fig. 1b,c).

The megaripple site was visited during two intensive field campaigns, in 2019 from 07 to 14 September and again in 2022 from 28 March to 06 April (hereafter referred to as April deployments). The water temperature varied less than 2°C during each campaign but had averages that differed almost 10°C between seasons (20.9°C in April vs. 30.4°C in September). From our AEC velocity measurements in the bottom water (max: 31 cm s^{-1}; Fig. 3a) and by assuming a log-velocity profile, we estimated that the current varied between 0 and ~ 60 cm s^{-1} in the surface water during our deployments.

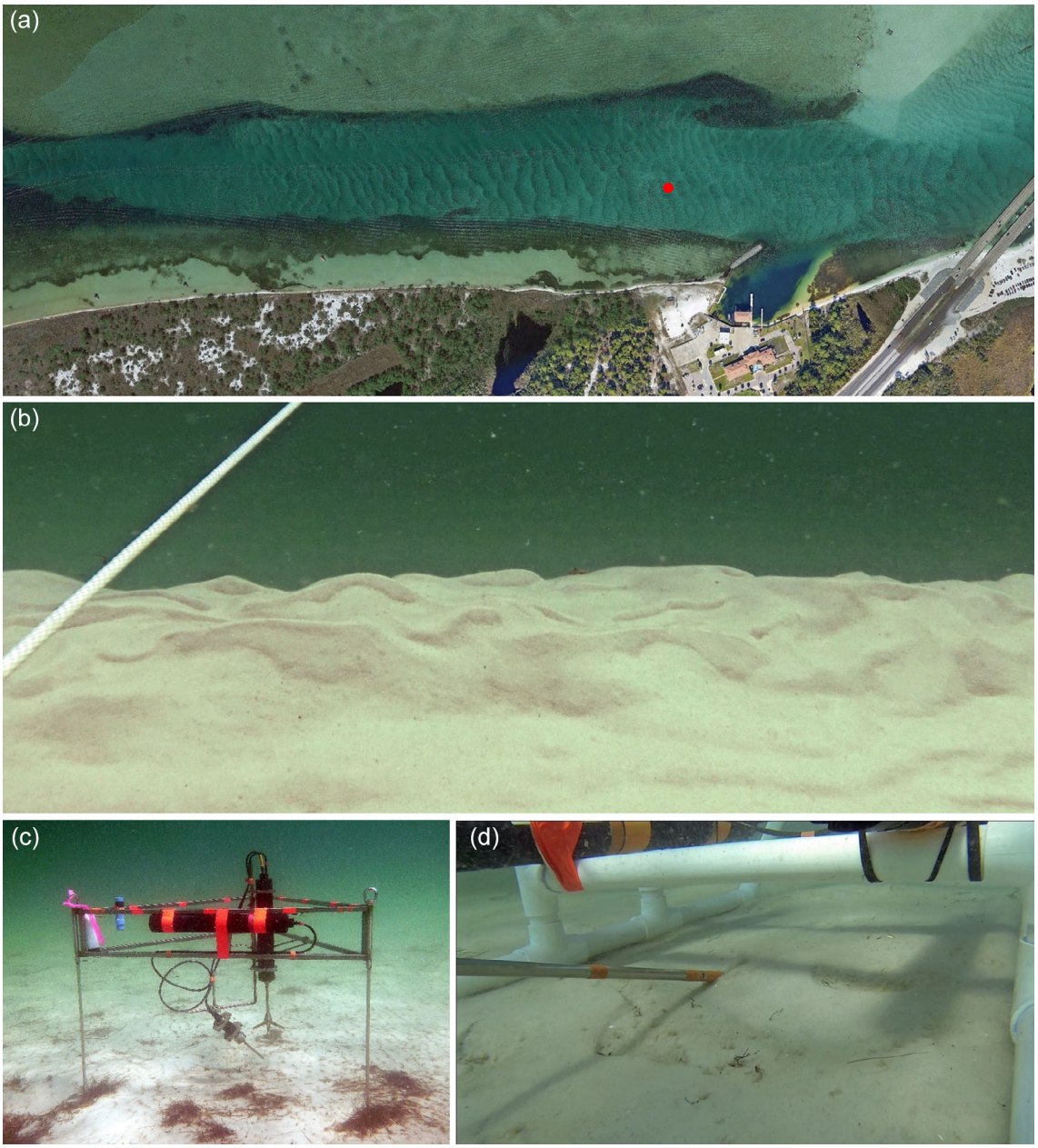

Fig. 1. Megaripple field and instruments deployed. (**a**) Google Earth image of the megaripple field in Destin, Florida, USA. For scale, *note* the four-lane highway and parked cars in bottom right corner. The average ripple wavelength was ~ 18 m. The United State Coast Guard Station Destin, FL, is seen in the lower part of the image. (**b**) Crest of a megaripple with smaller ripples superimposed. For scale, the rope is approximately 12-mm thick. (**c**) An aquatic eddy covariance system deployed over the permeable sandy bottom at the location marked with a red dot in (**a**). Small sand ripples and other rugosities are visible at the bottom. A light logger and a reference O_2 sensor are attached to the upper left corner of the instrument frame. (**d**) A 12-mm diameter stainless steel rod with a fast-responding optical O_2 sensor mounted in a protective groove to measure concentration in the top sediment layer. The rod was attached to a benthic sled that was pulled at slow speed by a boat through the megaripple field. All underwater images were captured with GoPro Hero 3+ cameras. *See* text for more details.

One or two identical AEC instruments were deployed during our field campaigns (Fig. 1c). Details on these instruments and how the fluxes were extracted from the raw measurements are given in the Supporting Information. An autonomous O_2 reference sensor and a photosynthetically active radiation (PAR) sensor were mounted on one of the AEC instrument frames (Fig. 1c). The two field campaigns produced over 600 high-quality O_2 flux estimates, each based on 15-min of AEC data.

Magnitudes and dynamics of O_2 fluxes were analyzed for influences of short- and long-term drivers. To compare results

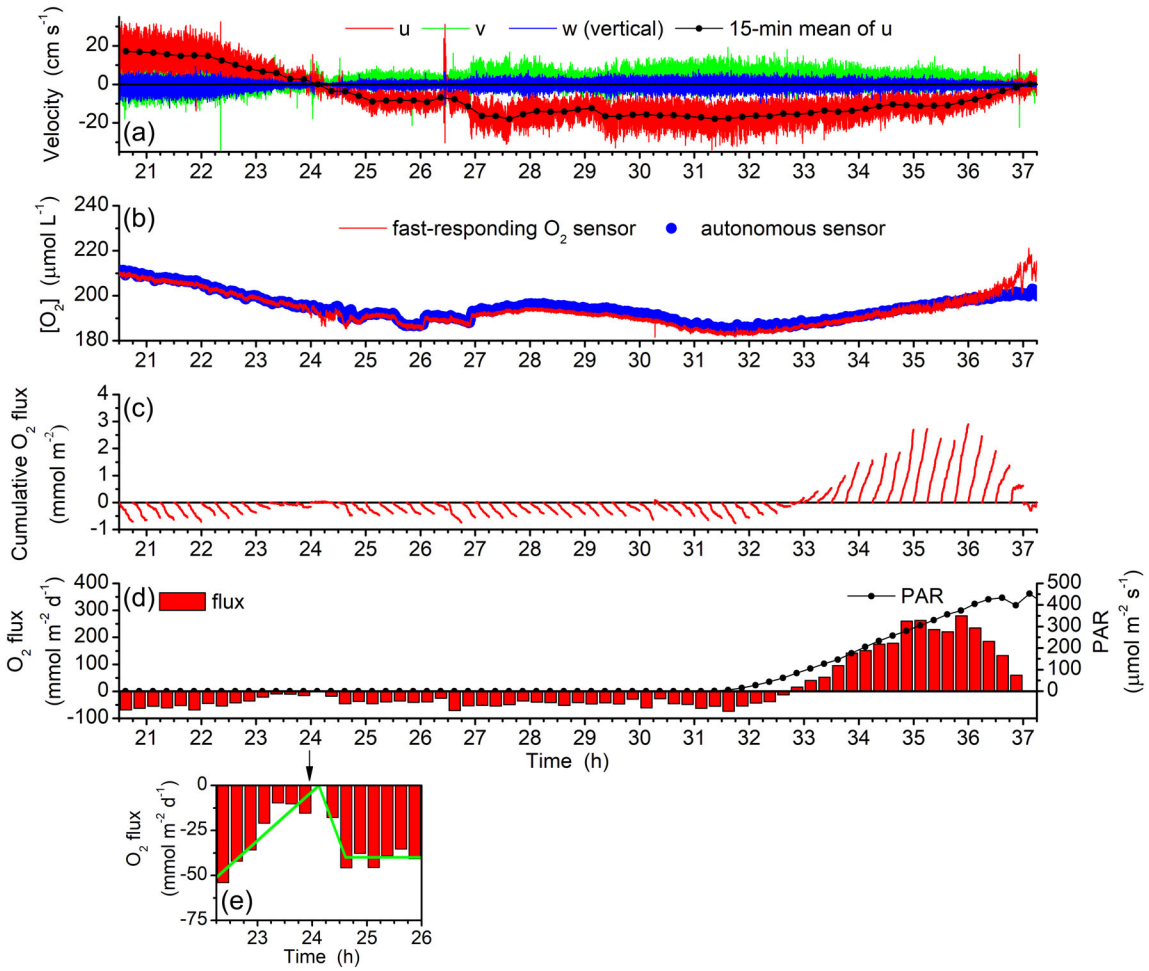

Fig. 2. Aquatic eddy covariance example deployment, 17-h long. (**a**) Three velocity components (*x*, *y*, *z*) and 15-min mean of the current velocity measured 14 cm above the bottom. Visible disturbances were caused by floating debris. (**b**) Concentrations measured by the O_2 sensor and the autonomous reference sensor. The diel O_2 cycle recorded by the two sensors agrees well except during the second slack tide when O_2 presumably was building up in the near-stagnant bottom water due to intense benthic primary production. (**c**) Cumulative O_2 fluxes for 15-min data segments used for flux extractions. The near-linear trends reveal a strong flux signal in the data. (**d**) O_2 fluxes for 15-min data segments and light (PAR) at the bottom. Positive fluxes represent a net release of O_2. (**e**) Close-up of O_2 fluxes around nighttime slack tide illustrating the strong modulation of the O_2 exchange in the megaripple by the current velocity.

of our two field campaigns with those reported from other shallow-water ecosystems, the O_2 fluxes for each campaign were averaged to generate 24 hourly fluxes and used to calculate daily respiration (R), gross primary production (GPP), and net ecosystem metabolism (NEM) as outlined by Hume et al. (2011) and Rheuban et al. (2014). Finally, the size of the footprint, the area on the sediment surface that gives 90% of the measured eddy flux, was calculated as described by Berg et al. (2007) and related to the extent of the megaripples.

Megaripple topography and O_2 concentration in the top sediment layer were measured from a benthic sled that was pulled slowly by a boat over the megaripple field (Fig. 1d). Relevant for the interpretation of the benthic O_2 fluxes, the variation of O_2 concentration in the sediment surface layer was used to assess the spatial variability of the sediment–water O_2 gradient in the megaripple field. The instruments used and details of these measurements are described in the Supporting Information.

Results

A general pattern in our flux measurements is that the sediment–water O_2 exchange in the megaripple field was relatively large in magnitude during both day- and nighttime, and highly dynamic. During the example deployment shown in Fig. 2, the nighttime O_2 uptake varied between 0 and -75 mmol m^{-2} d^{-1} as the tidal current, measured 14 cm above the sand, varied between $\pm$ 20 cm s^{-1} (Fig. 2a,d). The tight control the current had on the O_2 uptake is evident at

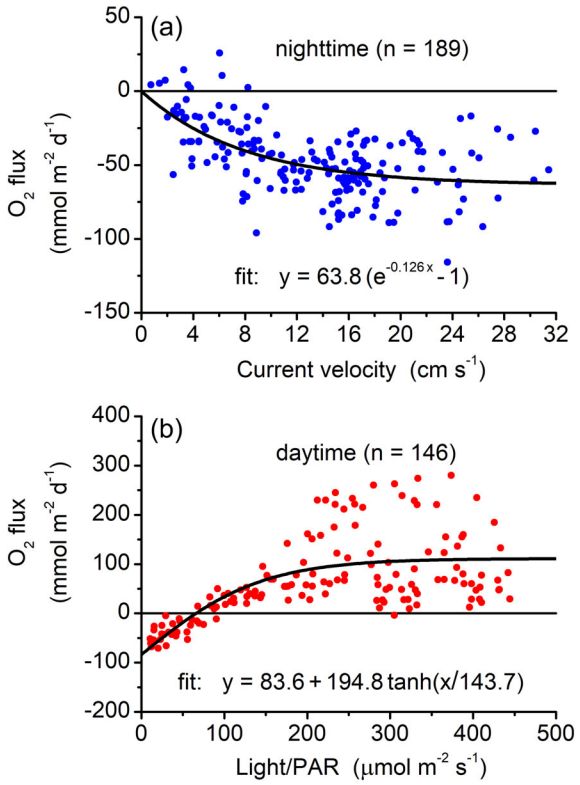

Fig. 3. Main short-term drivers of O_2 flux between the permeable megaripple sand and water column above. The fitted lines are derived from all 15-min fluxes measured during the September 2019 field campaign. (**a**) Nighttime O_2 flux vs. current velocity. The exponential fit shows that stimulation of O_2 uptake tapers off at high velocities. The large spread of the data illustrates that other environmental and dynamic drivers affect the benthic O_2 exchange. (**b**) Daytime O_2 flux vs. light. The well-known PI curve (Jassby and Platt 1976) modified to account for respiration and fitted to the data shows that the apparent light saturation of the production occurred at about half the maximum light levels measured at the bottom (*see* Discussion).

slack tide when O_2 uptake reached a minimum (Fig. 2e; time ~ 24 h). During daytime, an O_2 release of 300 mmol m^{-2} d^{-1} was measured as light levels approached their maximum (Fig. 2d) and while the current velocity remained substantial. As the current velocity diminished toward slack tide (Fig. 2a; time ~ 36.5 h), the measured daytime O_2 release dropped (Fig. 2d). This is presumably caused by reduced vertical current-driven mixing in the bottom water. The difference in concentration that occurred at that particular point in time between the eddy- and the autonomous reference O_2 sensor (Fig. 2b) positioned at different heights above the sand (14 vs. ~ 60 cm; Fig. 1c) suggest that photosynthetic production continued and that a substantial O_2 gradient formed in the lower water column due to reduced vertical mixing in the near-stagnant water. The size of the footprint for the measured O_2 fluxes were calculated to be 23-m long following the approach outlined by Berg et al. (2007).

Separating all the 15-min based O_2 fluxes from our September field campaign into night- and daytime values using a light threshold of 10 μmol m^{-2} s^{-1} and plotting and fitting these values as functions of current velocity (Fig. 3a) and light (Fig. 3b), underpins the dependencies of O_2 flux on current velocity and light. The relatively large spread in data around the fitted lines suggests that multiple environmental drivers and dynamic effects influenced the benthic O_2 exchange (*see* Discussion). Also, our data, measured under naturally varying environmental conditions, demonstrate a decrease in flow-stimulation of the O_2 uptake at high current velocities (Fig. 3a). Similar patterns were observed during the April campaign.

The key metabolic numbers, daily R, GPP, and NEM, were markedly different between the two field campaigns (Fig. 4a). R and GPP were 140% and 190% larger in September than in April. NEM amounted to 6.7 mmol m^{-2} d^{-1} in September and was practically zero in April. Because current velocity affects O_2 consumption during both day and night (Figs. 2, 3a), the mean velocity was calculated for each period (Fig. 4b). While the mean current velocity did not vary much between day and night or between our two field campaigns (Fig. 4b), both light levels (Fig. 4c) and water temperature (Fig. 4d) were considerably larger in September than in April, 69% and 45%, respectively. Relating the difference in R between our two field campaigns to temperature alone corresponds to a Q_{10} value of 2.5 (the factor a rate increases for any 10°C increase in temperature; $Q_{10} = (R2/R1)^{10/(T2 - T1)}$). The equivalent calculation for GPP gives a Q_{10} value of 3.1.

The megaripple topography measured from the benthic sled was modest when relating it to the entire water column (Fig. 5a vs. 5b). The min and max O_2 concentrations in the top sediment layer (Fig. 5c) did not vary significantly as revealed by the O_2 sensor attached to the sled that was pulled over the megaripple field (Fig. 1d). At all times, O_2 concentration was larger in the top sediment layer than in the water column as measured by the O_2 sensor 14 cm above the sand. This pattern is consistent with the near-constant O_2 release due to photosynthetic production measured concurrently by AEC (Fig. 5e). During these synchronous measurements, the bottom current was running at a steady velocity of 23 cm s^{-1} (Fig. 5d).

Discussion

Measuring benthic fluxes is a challenging task in high-energy settings such as the sand megaripple field studied here. During our field campaigns, we encountered strong surface currents of up to 60 cm s^{-1}, which transferred to the bottom and drove advective exchange between the highly permeable sand and the water column above (Figs. 2e, 3a). As the permeability of the sand is ~ 50 times higher than the threshold where advective exchange is considered to exceed molecular diffusion (5×10^{-11} vs. ~ 10^{-12} m^2; Huettel et al. 2014), current was the main driver of benthic exchange. As a result, traditional enclosure approaches such as in situ benthic

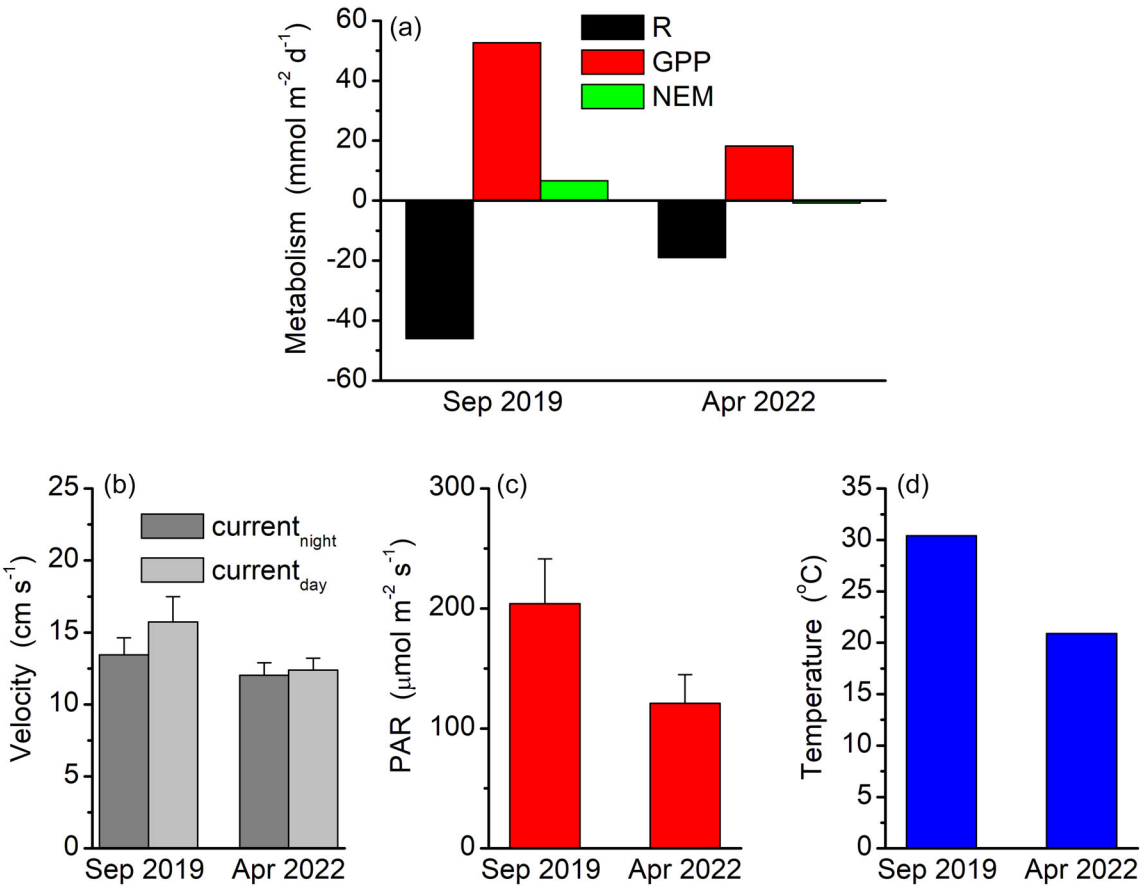

Fig. 4. Daily metabolic numbers and associated main drivers for the September 2019 and April 2022 field campaigns. All of our data for each campaign were averaged into 24 hourly composite values before the depicted numbers were calculated. (**a**) Daily respiration (R), gross primary production (GPP), and net ecosystem metabolism (NEM). Because these daily numbers were calculated from 24 hourly values no error estimates are available. (**b**) Mean (± SE) night- and daytime current velocities (September 2019: $n_{night} = n_{day} = 12$; April 2022: $n_{night} = 13$, $n_{day} = 11$). (**c**) Mean (± SE) light at the bottom. (**d**) Mean (± SE) bottom water temperature (error bars not visible).

chambers, which exclude all natural flow, would likely fail to give meaningful data that represent the natural benthic environment under the substantial current velocities that frequently are encountered at our study site (Berg et al. 2013; Attard et al. 2015). This was our main incentive for using the AEC technique for benthic O_2 flux measurements (Berg et al. 2003) as it does not suffer from this shortcoming.

When deploying our AEC instruments, we aimed at positioning them midway between megaripple crests (Fig. 5a,b). These areas are covered with small ripples and other rugosities (Fig. 1b,c). From the AEC measurements, we estimated the footprint of the O_2 exchange as outlined by Berg et al. (2007) to extend 23 m upstream from each instrument. The location of the footprint changed obviously with the direction of the tidally driven current, but as shown by Berg et al. (2007), its size was not dependent on the strength of the current. Thus, with a near-constant footprint size of 23 m and an average distance between the megaripple crests of ~ 18 m (Fig. 5a,b), we evaluate that our measured O_2 fluxes represent well the megaripple field as a whole, including contributions from areas of both crest and trough and areas covered with smaller sand ripples and other rugosities. This is supported by the fact that the O_2 concentration in the top sediment layer, measured from the sled that was pulled over the megaripple field, did not vary markedly relative to the water column concentration (Fig. 5c). In addition, this is also supported by two shorter exploratory AEC instrument deployments we made at the start of the study during the September 2019 campaign with a measuring height of 30 cm instead of the 14 cm used later. Fluxes from these initial deployments, which had a significantly larger footprint (61 vs. 23 m), were indistinguishable from those measured later.

Overall, the megaripple field was found to be an intense metabolic hotspot with an O_2 exchange ranging between a nighttime uptake of $-100\ mmol\ m^{-2}\ d^{-1}$ and a daytime release of $300\ mmol\ m^{-2}\ d^{-1}$ (Fig. 3). These rates are larger

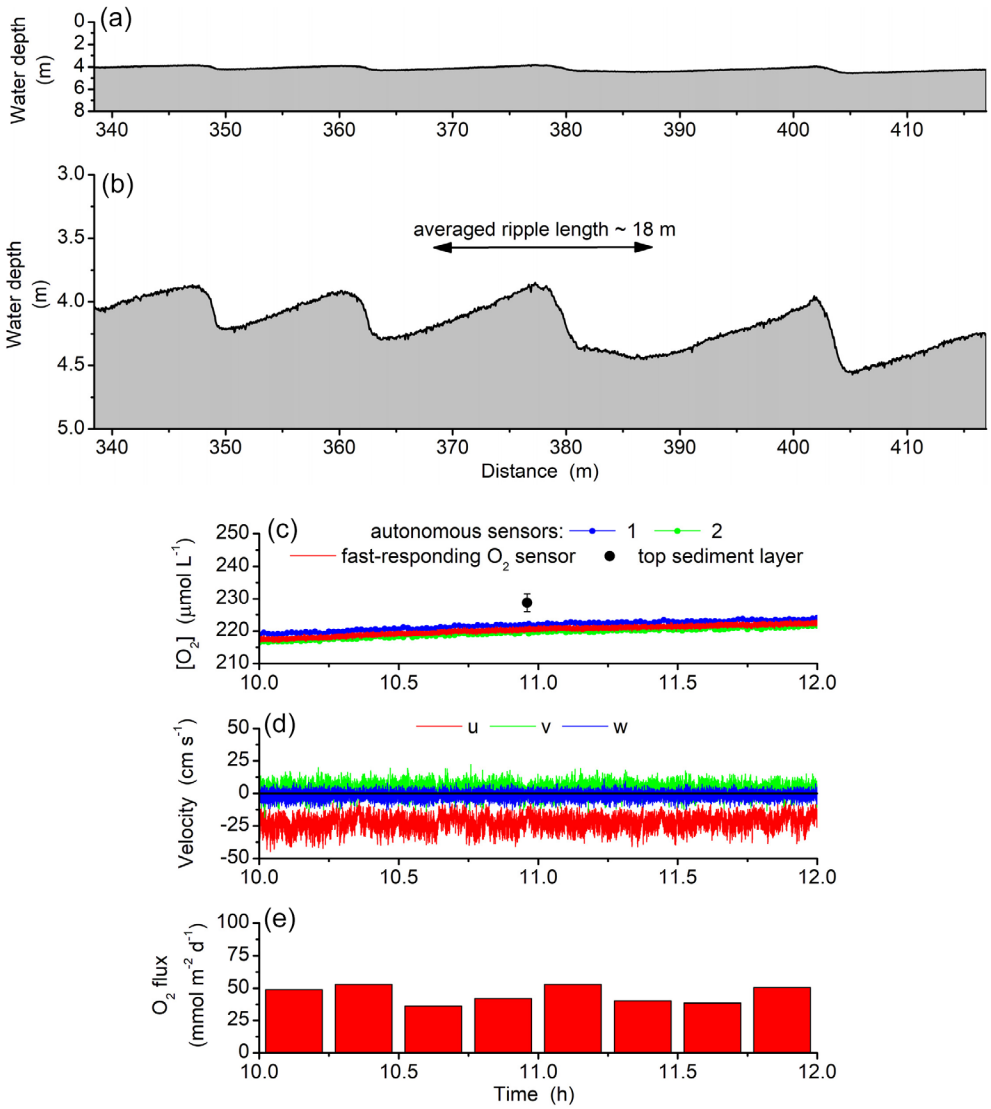

Fig. 5. Megaripple topography, O_2 concentration in the top sediment layer, and concurrent aquatic eddy covariance measurements. (**a**) The full water depth of ~ 4 m over the megaripple field and its topography shown using the same scale on *x*- and *y*-axis. (**b**) Same data, but with a finer scale used on the *y*-axis. (**c**) Concentrations measured with the O_2 sensor, two autonomous reference sensors, and the fast-responding optical O_2 sensor in the top sediment layer. The latter was mounted on a stainless steel rod and attached to a benthic sled pulled by a boat (Fig. 1d). The dot represents the measured mean and the "error bars" min- and max concentrations. (**d**) Three velocity components (*x*, *y*, *z*). The steady mean current velocity was 23 cm s^{-1}. (**e**) O_2 flux for 15-min data segments. Positive fluxes represent a net release of O_2.

than those typically found for near-shore sediments with water depths < 10 m (Glud 2008; Jørgensen et al. 2022). Also, the O_2 exchange of the megaripple sand was highly dynamic and appeared never to be at steady state due to constantly changing short-term drivers, mainly the tidally driven current over the bottom and light (Figs. 2, 3). The significant O_2 fluxes were presumably sustained by advective transport of O_2, nutrients, and organic matter (fuel) into or out of the highly permeable sand, and importantly, overlaid by rapid internal cycling. The notion that such substantial advective transport occurred is supported by the strong stimulation that current velocity had on the O_2 flux (Figs. 2e, 3a). Similarly, the presumption that rapid internal cycling occurred is supported by the fact that the ratio between daily R and GPP for our two field campaigns (Fig. 4) were close to 1 (0.9 vs. 1.0) despite large differences in R and GPP between these campaigns.

The megaripple appeared to be slightly autotrophic during the September campaign (NEM = 6.6 mmol m^{-2} d^{-1}) but practically in a metabolic balance during the April campaign (NEM = −0.8 mmol m^{-2} d^{-1}). However, given the highly dynamic nature of the benthic system, including its tight response to a change in drivers, these NEM values should not necessarily be seen as typical for the respective months or

seasons. A string of cloudy days in September for example could result in a negative NEM value, and thus, reflect heterotrophic conditions. In line with many other AEC studies (Berg et al. 2022), our results from this megaripple field, with its highly dynamic O_2 exchange, emphasize how important it is to rely on frequent measurements throughout the months or seasons to correctly assess the trophic status of shallow-water benthic ecosystems. This is particularly true for systems, as the one investigated here, that are close to being in metabolic balance.

With respect to long-term drivers, a seasonal decrease in temperature of 9.5°C (Fig. 4d) between September 2019 and April 2022 is likely the main reason for the 2.4-fold decrease in R (Fig. 4a). Relating this difference in R to temperature alone corresponds to a Q_{10} value of 2.5 which is in line with findings for other shallow-water marine sediments (Glud 2008). It is possible, however, that a fraction of this increase in R was linked through rapid internal cycling to the synchronous increase in GPP. Studies of phototrophic systems have shown that highly labile compounds produced as part of photosynthetic processes accumulate as the day progresses and are rapidly consumed during the following night (Juska and Berg 2022). The 2.9-fold greater GPP in September compared to April (Fig. 4a) is likely the result of two significant factors, namely the higher temperature, which alone corresponds to a Q_{10} value of 3.1, and the 69% increase in the mean light reaching the bottom (Fig. 4c). As a reference, measurements in diatom-covered sediments have shown a photosynthetic Q_{10} response of 2.2–2.6 (Hancke and Glud 2004). The fact that our Q_{10} of 3.1 is not far from that range and that the apparent light saturation occurs at about half the max light level measured over the megaripple field (Fig. 3b), suggests that most of the September to April increase in GPP is temperature related. The complex interplay captured in AEC measurements between various drivers of benthic O_2 exchange, some of them with very different timescales, makes it challenging to accurately pinpoint their relative importance.

The external input of organic matter (fuel) to the sediment is the ultimate driver of benthic O_2 exchange. A lack of organic matter input will lead to diminishing O_2 exchange that eventually will approach zero. Permeable sediments allow advective entrainment of both particulate and dissolved compounds (Huettel et al. 2014), which is an additional mechanism for receiving organic matter compared to muddy cohesive sediment. In that light it is not surprising that permeable sands often have higher O_2 uptake than muddy sediments—a fact that is still not fully recognized. The opposing, but faulty, view was common years ago and was rooted in the fact that sands often have a lower organic matter content than muddy sediment, combined with earlier limited means to measure O_2 exchange for permeable sands under naturally varying environmental conditions. This AEC study of a shallow-water megaripple field adds to the supposition that most permeable sandy sediments are metabolically highly active sites.

To our knowledge, the results presented here are the first of their kind to quantify O_2 dynamics and carbon cycling in a megaripple field. Our measurements were done in shallow-water megaripples, but as the same entrainment of bottom water and resulting capturing of organic matter happens at any water depths, we cautiously propose that megaripples in deeper waters act as metabolic hotspots too. Given how widespread megaripples are in high-energy marine settings, they have the potential to impact the carbon budget for the ecosystems where they are found. More research of megaripples in deeper waters below the photic zone is needed to address this question more quantitatively.

References

Ashley, G. M. 1990. Classification of large-scale subaqueous bedforms; a new look at an old problem. J. Sediment. Res. **60**: 160–172. doi:10.2110/jsr.60.160

Attard, K. M., H. Stahl, N. A. Kamenos, G. Turner, H. L. Burdett, and R. N. Glud. 2015. Benthic oxygen exchange in a live coralline algal bed and an adjacent sandy habitat: An eddy covariance study. Mar. Ecol. Prog. Ser. **535**: 99–115. doi:10.3354/meps11413

Attard, K. M., I. F. Rodil, R. N. Glud, P. Berg, J. Norkko, and A. Norkko. 2019. Seasonal ecosystem metabolism across shallow benthic habitats measured by aquatic eddy covariance. Limnol. Oceanogr.: Lett. **4**: 79–86. doi:10.1002/lol2.10107

Bellec, V. K., V. R. Van Lancker, K. Degrendele, M. Roche, and S. Le Bot. 2010. Geo-environmental characterization of the Kwinte Bank. J. Coast. Res. **51**: 63–76. doi:10.2112/si51-006.1

Bellec, V. K., and others. 2019. Sandbanks, sandwaves and megaripples on Spitsbergenbanken, Barents Sea. Mar. Geol. **416**: 105998. doi:10.1016/j.margeo.2019.105998

Berg, P., and others. 2003. Oxygen uptake by aquatic sediments measured with a novel non-invasive eddy-correlation technique. Mar. Ecol. Prog. Ser. **261**: 75–83. doi:10.3354/meps261075

Berg, P., H. Roy, and P. L. Wiberg. 2007. Eddy correlation flux measurements: The sediment surface area that contributes to the flux. Limnol. Oceanogr. **52**: 1672–1684. doi:10.4319/lo.2007.52.4.1672

Berg, P., and others. 2013. Eddy correlation measurements of oxygen fluxes in permeable sediments exposed to varying current flow and light. Limnol. Oceanogr. **58**: 1329–1343. doi:10.4319/lo.2013.58.4.1329

Berg, P., M. Huettel, R. N. Glud, C. E. Reimers, and K. M. Attard. 2022. Aquatic eddy covariance: The method and its contributions to defining oxygen and carbon fluxes in marine environments. Ann. Rev. Mar. Sci. **14**: 431–455. doi:10.1146/annurev-marine-042121-012329

Boudreau, B. P., and others. 2001. Permeable marine sediments: Overturning an old paradigm. EOS **82**: 133–136. doi:10.1029/EO082i011p00133-01

Cacchione, D. A., M. E. Field, D. E. Drake, and G. B. Tate. 1987. Crescentic dunes on the inner continental-shelf off northern California. Geology **15**: 1134–1137. doi:10.1130/0091-7613(1987)15<1134:CDOTIC>2.0.CO;2

Carling, P. A. 1999. Subaqueous gravel dunes [review]. J. Sediment. Res. **69**: 534–545. doi:10.2110/jsr.69.534

Cheng, C. H., K. Soetaert, and B. W. Borsje. 2020. Sediment characteristics over asymmetrical tidal sand waves in the Dutch North Sea. J. Mar. Sci. Eng. **8**: 409. doi:10.3390/jmse8060409

Collins, M., S. Shimwell, S. Gao, H. Powell, C. Hewitson, and J. Taylor. 1995. Water and sediment movement in the vicinity of linear sandbanks: The Norfolk banks, southern North Sea. Mar. Geol. **123**: 125–142. doi:10.1016/0025-3227(95)00010-V

Cuevas, E., M. de los Ángeles Liceaga-Correa, L. A. Rincón-Sandoval, G. Mexicano-Cíntora, L. Arellano-Méndez, J. I. Euán-Ávila, H. Hernández-Núñez, and S. Mulsow. 2013. Morphological and sedimentological assessment of submarine dune fields on the coast of Yucatan, Mexico. Cienc. Mar. **39**: 83–99. doi:10.7773/cm.v39i1.2152

Engelund, F., and J. Fredsoe. 1982. Sediment ripples and dunes. Ann. Rev. Fluid Mech. **14**: 13–37. doi:10.1146/annurev.fl.14.010182.000305

Gallagher, E. L. 2003. A note on megaripples in the surf zone: Evidence for their relation to steady flow dunes. Mar. Geol. **193**: 171–176. doi:10.1016/S0025-3227(02)00662-X

Glud, R. N. 2008. Oxygen dynamics of marine sediments. Mar. Biol. Res. **4**: 243–289. doi:10.1080/17451000801888726

Hancke, K., and R. N. Glud. 2004. Temperature effects on respiration and photosynthesis in three diatom-dominated benthic communities. Aquat. Microb. Ecol. **37**: 265–281. doi:10.3354/ame037265

Huettel, M., and G. Gust. 1992. Impact of bioroughness on interfacial solute exchange in permeable sediments. Mar. Ecol. Prog. Ser. **89**: 253–267. doi:10.3354/meps089253

Huettel, M., W. Ziebis, and S. Forster. 1996. Flow-induced uptake of particulate matter in permeable sediments. Limnol. Oceanogr. **41**: 309–322. doi:10.4319/lo.1996.41.2.0309

Huettel, M., P. Berg, and J. E. Kostka. 2014. Benthic exchange and biogeochemical cycling in permeable sediments. Ann. Rev. Mar. Sci. **6**: 29–51. doi:10.1146/annurev-marine-051413-012706

Hume, A. C., P. Berg, and K. J. McGlathery. 2011. Dissolved oxygen fluxes and ecosystem metabolism in an eelgrass (*Zostera marina*) meadow measured with the eddy correlation technique. Limnol. Oceanogr. **56**: 86–96. doi:10.4319/lo.2011.56.1.0086

Iacono, C. L., and J. Guillén. 2008. Environmental conditions for gravelly and pebbly dunes and sorted bedforms on a moderate-energy inner shelf (Marettimo Island, Italy, western Mediterranean). Cont. Shelf Res. **28**: 245–256. doi:10.1016/j.csr.2007.08.005

Jassby, A. D., and T. Platt. 1976. Mathematical formulation of the relationship between photosynthesis and light for phytoplankton. Limnol. Oceanogr. **21**: 540–547, doi:10.4319/lo.1976.21.4.0540

Jørgensen, B. B., F. Wenzhöfer, M. Egger, and R. N. Glud. 2022. Sediment oxygen consumption: Role in the global marine carbon cycle. Earth-Sci. Rev. **228**: 103987. doi:10.1016/j.earscirev.2022.103987

Juska, I., and P. Berg. 2022. Variation in seagrass meadow respiration measured by aquatic eddy covariance. Limnol. Oceanogr.: Lett. **7**: 410–418. doi:10.1002/lol2.10276

Long, M. H. 2021. Aquatic biogeochemical Eddy covariance fluxes in the presence of waves. J. Geophys. Res.: Oceans **126**: e2020JC016637. doi:10.1029/2020JC016637

Lorrai, C., D. F. McGinnis, P. Berg, A. Brand, and A. Wüest. 2010. Application of oxygen eddy correlation in aquatic systems. J. Atmos. Oceanic Tech. **27**: 1533–46. doi:10.1175/2010JTECHO723.1

Poppe, L. J., S. J. Williams, M. S. Moser, N. A. Forfinski, H. F. Stewart, and E. F. Doran. 2008. Quaternary geology and sedimentary processes in the vicinity of six mile reef, eastern Long Island sound. J. Coast. Res. **24**: 255–266. doi:10.2112/06-0743.1

Rheuban, J. E., and P. Berg. 2013. The effects of spatial and temporal variability at the sediment surface on aquatic eddy correlation flux measurements. Limnol. Oceanogr. Methods **11**: 351–9. doi:10.4319/lom.2013.11.351

Rheuban, J. E., P. Berg, and K. J. McGlathery. 2014. Multiple timescale processes drive ecosystem metabolism in eelgrass (*Zostera marina*) meadows. Mar. Ecol. Prog. Ser. **507**: 1–13. doi:10.3354/meps10843

van Dijk, T. A., and M. G. Kleinhans. 2005. Processes controlling the dynamics of compound sand waves in the North Sea, Netherlands. J. Geophys. Res.: Earth Surf. **110**: 1–15. doi:10.1029/2004JF000173

Ziebis, W., M. Huettel, and S. Forster. 1996. Impact of biogenic sediment topography on oxygen fluxes in permeable seabeds. Mar. Ecol. Prog. Ser. **140**: 227–237. doi:10.3354/meps140227

Acknowledgments

This work was funded by the National Science Foundation through grants to Peter Berg (OCE-1851424) and Markus Huettel (OCE-1851290, OCE-2148635), and by the University of Virginia and Florida State University. We thank the United States Coast Guard Station Destin, FL, for allowing us to operate from their premises during field campaigns. We finally thank Clare Reimers and an anonymous reviewer for detailed and insightful comments that have improved the manuscript.

Submitted 30 January 2023
Revised 24 June 2023
Accepted 27 June 2023